Analysis of Poly(ethylene glycol) from the Conservation of 17th Century Shipwreck *Vasa* and Associated Wooden Objects.

Brennan J. Curole[1], Malin Sahlstedt[2], Scott M. Grayson[1*]

[1] *Department of Chemistry, Tulane University, New Orleans, LA 70118, United States*

[2] *Vasa Museum, Swedish National Maritime Museums, Stockholm, Sweden*

Abstract

Vasa, a Swedish warship that sunk in 1628 and was excavated in 1961, and associated wooden objects underwent a preservation process using various low molecular weights (600, 1500, and 4000 M_n) of poly(ethylene glycol) (PEG) to gradually displace the water within the wooden structure, preventing the collapse of the waterlogged wood upon drying. However, after six decades of aging after application, to what extent are these polymers degraded? To investigate this, a Soxhlet apparatus was used to extract PEG from wooden samples of *Vasa*, and lyophilization was used to dry aqueous PEG solutions, these samples being the runoff accumulated during the application of different molecular weights of PEG to *Vasa* and other associated wooden objects. These samples underwent analysis via matrix-assisted laser desorption/ionization – time-of-flight mass spectrometry (MALDI-TOF MS), gel permeation chromatography (GPC), and ^{1}H and ^{13}C nuclear magnetic resonance (NMR) spectroscopy.

The primary discovery was that the PEG within *Vasa* exhibited minimal degradation, with the dominant identified species, as determined by MALDI-TOF MS and NMR spectroscopy, being HO-PEG-OH. However, small quantities of HO-PEG-OH had undergone degradation, resulting in the formation of PEG chains with distinct end groups, notably a range of carbonyl-

based compounds, including aldehydes, carboxylic acids, and esters, as observed through MALDI-TOF MS, ^{1}H, and ^{13}C-NMR spectroscopy. These mass spectrometry product peaks could be confirmed by the expected mass difference through various end-group functionalizations, such as oxidations, esterifications, or ether formations. In addition to the carbonyl-based degradation products, some PEG chains had completely cleaved into two separate lower molecular weight HO-PEG-OH polymers, each approximately half of their original molecular weight, as revealed by GPC analysis.

Key Words: Poly(ethylene glycol) (PEG), Oxidative degradation, MALDI-TOF MS, *Vasa*

1. Introduction

Poly(ethylene glycol) (PEG), also known as poly(ethylene oxide) (PEO) when molecular weight > 150,000 Da, is a synthetic polyether that is available in a wide variety of molecular weights and architectures. Due to its hydrophilicity, nontoxicity, and low cost, PEG is used in a variety of industrial, medical, and commercial applications. For instance, it has been used as a three-dimensional scaffold for the growth of neural cells,[1] a common additive in cosmetic products,[2] and a solid-state electrolyte for lithium metal batteries.[3]

Additionally, PEG has been used as an agent in the preservation of waterlogged wooden artifacts, specifically excavated shipwrecks, like *Vasa*,[4–8] *Bremen Cog*,[9–11] *Batavia*,[12] and *Mary Rose*.[13–15] Prior to 1959, creosote and linseed oil, carboxymethyl cellulose, or alum (potassium aluminum sulfate) were all typically used in the preservation of waterlogged wood; however, many objects preserved with these techniques have sustained damage through chemical or mechanical stress that in some cases have led to material or complete object loss.[4] Between 1957

and 1960, preliminary results on *Vasa* showed that 4000 molecular weight PEG penetrated the wood and prevented shrinkage more effectively than other techniques available at the time so 4000 M_n was applied to *Vasa* over the course of many years to prevent further damage to the ship.[4] A 4000 M_n PEG solution in water was the first to be applied to the ship, however, it hadn't completely penetrated to the inner bulk of the wood, so this was followed by 1500 and 600 M_n solutions of PEG in the following years. The switch to lower molecular weights of PEG was influenced by continued research results indicating that lower molecular weights of PEG had better diffusion into wood and even the ability to bond with the timber's cell walls directly thus improving dimensional stability.[4]

While PEG is used in a variety of applications, including medicine,[16,17] cosmetics,[2,18] and food packaging,[19,20] it can experience degradation under more extreme conditions[21] including: moderate heating,[22,23] microbiological exposure,[24] oxidative conditions,[25] and autooxidation.[26] These degradation products can possibly pose issues in terms of both toxicity (in the case of pharmaceutical applications)[27] and the formation of secondary reactive species[28] which can lead to the continued degradation of the PEG itself, or, in the case of *Vasa*, the wood.[5]

In this work, three samples of PEG that were impregnated in *Vasa's* wood, from the forwarded part of the ship's hull, were extracted and analyzed to measure the degree of their deterioration and the products of their degradation. Selective end-group functionalizations were used to track mass differences. Matrix-assisted laser desorption ionization time-of-flight mass spectrometry (MALDI-TOF MS), gel permeation chromatography (GPC), and nuclear magnetic resonance (NMR) spectroscopy were used to identify the molecular weights of the polymers and confirm the presence of certain functional groups.

2. Experimental

2.1 Materials

There are three different sets of PEG samples in this work. The first of which were the runoff of the solubilized preservation PEG samples. These samples include **65943**: PEG 600 M_n Borax (boric acid 1-2%) and **65946**: PEG 1500 M_n (approximately 15% PEG in water), which are the remnants collected during the application of PEG to *Vasa* (sometime between 1962 to 1970), plus **65942**: PEG 4000 M_n ca 45%, **65944**: PEG 1500 M_n ca 50%, and **65945**: PEG 4000 M_n ca 40% which are the run-off of the PEG samples that were used in large, heated baths to impregnate smaller wooden objects associated with *Vasa* (before 1970). It should be noted that these solutions (**65942** – **65946**) were recirculated and reused a number of times in the preservation of *Vasa* and associated wooden objects. Due to this recirculation, it is possible that metal ion contaminants from iron containing parts of the ship were spread amongst the surface of the rest of the ship. The next PEG samples were the three that were impregnated in wood and were extracted from small adjacent pieces of *Vasa* planking (**65947**, **65948**, and **65949**). Lastly, the modern-day PEG references of 600 M_n (Sigma Aldrich), 1500 M_n (Sample from The Western Australian Museum provided by Vicki Richards), and 4000 M_n (Alfa Aesar). The samples will be referred to as either preservation PEGs, extracted PEGs, or reference PEGs, respectively, throughout the paper. *Vasa* samples **65942**-**65949** were acquired from Malin Sahlstedt in collaboration with *Vasamuseet* in Stockholm, Sweden. Dichloromethane (DCM), diethyl ether (DEE), chloroform, sodium hydroxide, and monobasic sodium phosphate were obtained from Fisher Scientific. Isopropyl alcohol (IPA) was obtained from Pharmco. Potassium permanganate was obtained from General Chemical Company. Tetrahydrofuran (THF) was obtained by Honeywell. Hydrochloric acid was obtained from VWR. Triethylamine was

obtained from TCI. Benzyl bromide, magnesium sulfate, sodium sulfite, methanesulfonyl chloride, and 4-(dimethylamino)pyridine (DMAP) were obtained from Sigma Aldrich. Sodium hydride, 60% dispersion in mineral oil was obtained from Acros Organics and was washed with hexanes to remove the mineral oil before use. All other chemicals were used without further purification.

2.2 Extraction

Extraction of the solubilized preservation PEG samples (**65942-65946**) from water was achieved by lyophilization. Two milliliters of each preservation PEG solution were diluted to 10 milliliters with deionized water, homogenized, to ensure even freezing, and lyophilized for 24 hours. While these samples had estimates of their respective PEG concentrations ranging from 40 to 50%, it was found that, by mass/volume, the samples contained anywhere from 23 to 55% PEG (**Table 1**). Collection of the extracted PEG from the impregnated *Vasa* planking (samples **65947**, **65948**, and **65949**) was achieved via Soxhlet extraction with chloroform. The samples of wood from the planking (**65947-65949**) weighed approximately 6 to 7 grams and were cut into pieces with a small hacksaw. Portions between 1.5 and 2.0 grams were placed in a Soxhlet extractor with 200 mL of chloroform as the extracting solvent, and oxygen was removed from the system via 3 freeze, pump, thaw cycles. The apparatus was backfilled with argon gas to avoid atmospheric oxidation, covered with aluminum foil to avoid photoreactions, and placed in an oil bath that was heated to 85 ˚C to achieve vigorous boiling. The solution was refluxed for 24 hours and allowed to cool to room temperature before it was removed. The extracted chloroform solution was dried with magnesium sulfate, and the solvent was removed under reduced pressure. The three wooden samples yielded an extract (predominantly PEG) between 47.3% to

54.6% of their preliminary masses (wood + PEG) (**Table 2**). These samples were mixtures of various molecular weights of HO-PEG-OH, but they were primarily composed of dispersed 600, 1500, and 4000 M_n PEG distributions.

Sample Name	Volume of PEG Solution (mL)	Mass of Dry Sample (g)	Mass/Volume % Concentration
65942: PEG 4000 M_n ca 45	2	0.975	48.7%
65943: PEG 600 M_n Borax (boric acid 1-2%)	2	0.942	47.1%
65944: PEG 1500 M_n ca 50%	2	1.105	55.3%
65945: PEG 4000 M_n ca 40%	2	0.679	34.0%
65946: PEG 1500 M_n ca 15%	2	0.461	23.1%

Table 1: Mass/volume % concentration of the recovered products from the aqueous *Vasa* samples after lyophilization.

Sample Name	Sample Mass (g)	Extract Mass (g)	Mass % of Extract
65947	1.4967	0.8169	54.6%
65948	1.7048	0.9172	53.8%
65949	1.9289	0.9122	47.3%

Table 2: Masses of the section cut from each complete wooden sample before extraction, masses of dried chloroform fraction recovered from each extraction, and mass percentages of dried chloroform fractions in the extracted samples.

The three wooden sample were taken from a larger piece of the forward part of the ship's hull (**Fig. 1**). Two of the resulting samples that were removed had only one face exposed to the exterior of the sample (**65948** and **65949**), where PEG was directly applied, and 5 subsequent faces that were not externally exposed. Sample **65947** had two of its faces to the exterior of the sample and only 4 subsequent faces that were not externally exposed. For the sake of consistency, each piece of wood that was removed from samples **65947**, **65948**, and **65949** to undergo Soxhlet extraction were removed from the same orientation with respect to one another. Each piece was removed from the top left corner of the sample.

Fig. 1. Larger wooden *Vasa* sample from which *Vasa* samples **65947**, **65948**, and **65949** were removed.

2.3 Selective Functionalizations

Acetylation of *Vasa* PEG via esterification

Extracted PEG from *Vasa* sample **65948** (106 mg, 0.18 mmol, 1 eq), acetic anhydride (0.37 ml, 3.53 mmol, 20 eq (10 eq per alcohol]), DMAP (47.5 mg, 0.39 mmol, 2.2 eq [1.1 eq per alcohol]), and DCM (5 mL) were added to a 20 mL scintillation vial and stirred overnight. The crude reaction solution was used for MALDI-TOF MS analysis.

Benzylation of *Vasa* PEG via Williamson Ether Synthesis

Extracted PEG from *Vasa* sample **65948** (135 mg, 0.23 mmol, 1 eq) was dried under vacuum at 60 ˚C for 4 hours in a flame dried 25 mL two-neck round-bottomed flask. The extract was cooled, the flask was backfilled with Ar gas, and dry THF (~10 mL) was added to the flask via cannula. Sodium hydride (22 mg, 0.90 mmol, 4 eq [2 eq per alcohol]) was added to the flask and benzyl bromide (0.21 mL, 1.8 mmol, 8 eq [4 eq per alcohol]) was injected into the reaction solution and stirred overnight. The reaction solution was quenched with IPA (5 mL), and the solvent was removed via reduced pressure. The product was solubilized in water (5 mL) and was washed with DEE (3x 10 mL) to remove excess benzyl bromide. The product was extracted into DCM (3x 10 mL). The organic layers were combined and dried with anhydrous magnesium sulfate. The solvent was removed under reduced pressure, and the product was used for MALDI-TOF MS analysis.

2.4 Characterization

Gel permeation chromatography (GPC) was performed with a Waters Model 1515 isocratic pump a Waters Model 2414 differential refractometer detector (Waters Corp., Milford, MA), with four columns in series: a PSS SDV guard 3 mm (8 × 50 mm) and 3x PSS SDV analytical 500 Å (8 × 300 mm) 100 to 30,000 Da (Polymer Laboratories Inc., Amherst, MA). Data was collected in THF at a flow rate of 1 mL/min at 25 °C for 45 min. M_n, M_w, and Đ values were calibrated against PEG standards from Polymer Laboratories.

A Bruker Autoflex III MALDI-TOF mass spectrometer (Bruker Daltonics, Billerica, MA) and Bruker UltrafleXtreme MALDI-TOF mass spectrometer (Bruker Daltonics, Billerica, MA) were used to collect data. Mass spectral data were collected in positive reflector ion detection mode. The typical sample preparation for MALDI-TOF MS data was performed using

stock solutions in tetrahydrofuran (THF) of the matrix (20 mg/mL), polymer analyte (2 mg/mL), and a cation source (2 mg/mL). The stock solutions were combined in a 20/5/1 ratio (v/v/v) (matrix/analyte/cation), and 1 μL was plated via the dried droplet method. Sodium trifluoroacetate (Sigma) was used as the cation source, and *trans*-2-[3-(4-*tert*-butylphenyl)-2-methyl-2-propenylidene]malononitrile (DCTB) was used as the matrix in the sample preparation. MALDI-TOF MS spectra were calibrated against SpheriCal dendritic calibrants (Polymer Factory, Sweden).

Nuclear magnetic resonance (NMR) spectroscopy and heteronuclear single quantum coherence (HSQC) ^{1}H–^{13}C 2D-NMR spectroscopy was performed on a Bruker Avance Neo 400 MHz spectrometer and a Varian Unity Inova 400 MHz spectrometer (^{1}H (400 MHz), ^{13}C (101 MHz)). Experiments were performed at ambient probe temperature at a concentration of 100-300 mg/mL in chloroform-d ($CDCl_3$), purchased from Cambridge Isotope Laboratories (Andover, MA, USA). Sufficient scans were acquired to generate an adequate signal to noise with a relaxation delay of 5 s.

3. Results and Discussion

3.1 GPC Data

GPC was preliminarily used to measure the aqueous preservation of the PEG samples. GPC offers a particularly useful insight for these possibly complex mixtures. While the average masses of the aqueous preservation PEG samples were reported to be either 4000, 1500, or 600 Da with their respective estimated molecular weights, small amounts of the remaining two molecular weights were found in each **(Fig. 2)**. The retention times of the various molecular weight ranges being 19.0 – 23.0 minutes for ~4000 Da molecular weight species, 23.0 – 26.0

minutes for ~1500 Da molecular weight species, and 25.5 – 30.5 minutes for ~600 Da molecular weight species with a low molecular weight peak following a retention time of roughly 31 minutes. The following samples were measured via GPC and follow the naming format of [**code** (description of sample), M_n, M_w and Đ]: **65942** (PEG 4000 M_n ca 45%), M_n = 4050, M_w = 4530, and Đ = 1.12; **65943** (PEG 600 M_n Borax (boric acid 1-2%)), M_n = 760, M_w = 1120, and Đ = 1.47; **65944** (PEG 1500 M_n ca 50%), M_n = 1330, M_w = 1840, and Đ = 1.38; **65945** (PEG 4000 M_n ca 40%), M_n = 3750, M_w = 4370, and Đ = 1.17; **65946** (PEG 1500 M_n ca 15%), M_n = 1450, M_w = 1600, and Đ = 1.10). Due to limitations from the time of preservation, it is impossible to know the true initial M_n or dispersity of the original PEG samples that were initially used in the conservation effort, so the lyophilized preservation samples are referred to as 4000, 1500, and 600 M_n PEGs throughout the paper.

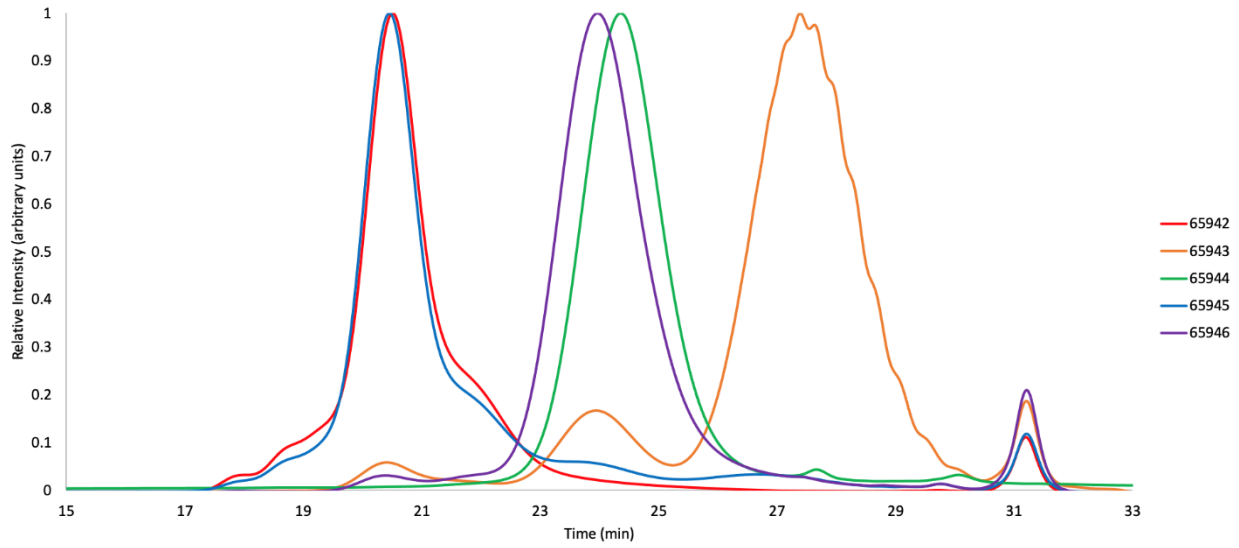

Fig. 2: GPC traces from lyophilized preservation samples (**65942**: PEG 4000 M_n ca 45%, M_n = 4050, M_w = 4530, and Đ = 1.12; **65943**: PEG 600 M_n Borax (boric acid 1-2%), M_n = 760, M_w = 1120, and Đ = 1.47; **65944**: PEG 1500 M_n ca 50%, M_n = 1330, M_w = 1840, and Đ = 1.38; **65945**:

PEG 4000 M_n ca 40%, M_n = 3750, M_w = 4370, and Đ = 1.17; **65946**: PEG 1500 M_n ca 15%, M_n = 1450, M_w = 1600, and Đ = 1.10) in THF.

Extracted PEG from the wooden samples were also analyzed via GPC **(Fig. 3)**. As expected, these samples are largely PEG and contain a mixture of molecular weights (4000, 1500, and 600 Da) at various concentrations. It was expected that the lower molecular weight PEGs would be the highest in concentration due to their ability to permeate into the timbers more effectively than the higher molecular weights of PEG.

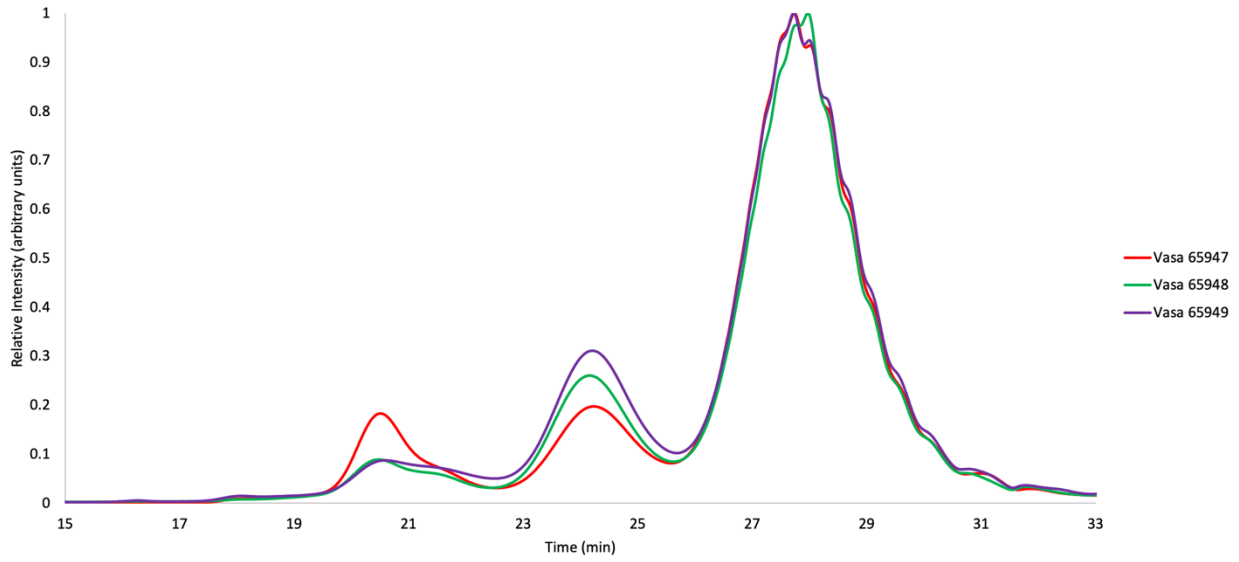

Fig. 3: GPC traces of extracted PEG from the wooden samples (**65947**: M_n = 910, M_w = 1960, and Đ = 2.15; **65948**: M_n = 830, M_w = 1630, and Đ = 1.96; and **65949**: M_n = 850, M_w = 1610, and Đ = 1.89) in THF.

These GPC traces were compared to modern reference HO-PEG-OH samples (labeled 4000, 1500, and 600 M_n) to investigate the difference in retention time and dispersity of *Vasa* PEG peaks. This difference can be attributed to either a loss of high molecular weight PEG

species via degradation and/or the formation of lower molecular weight PEG degradation products **(Fig. 4, S1**, and **S2)**. While these reference PEG samples were labeled as 4000, 1500, and 600 M_n, GPC and MALDI-TOF MS characterization were performed to get their actual M_n values. The reference PEG samples were run in triplicate over the course of multiple weeks to account for instrument variations with time. The reference PEG sample labeled as 4000 M_n was calculated to have an M_n of 4400 via GPC and 4200 via MALDI-TOF MS. The reference PEG sample labeled as 1500 M_n was calculated to have an M_n of 1500 via GPC and 1500 via MALDI-TOF MS, and the reference PEG sample labeled as 600 M_n was calculated to have an M_n of 600 via GPC and 660 via MALDI-TOF MS.

The extracted PEG *Vasa* samples were compared to the undegraded reference PEG analogues by measuring the difference of the areas under the curves between various points along the GPC trace. For this comparison, the total area under the peaks was normalized with respect to each corresponding mass range (4000, 1500, and 600 Da). The GPC traces were superimposed, and the loss of high molecular weight precursor and formation of low molecular weight products were calculated (**Fig. 4**). The two values calculated (percent loss of higher molecular weight PEG precursor and percent formation of lower molecular weight PEG products) were averaged for each sample and molecular weight range to give over all degradation profiles for each sample (**Fig. 5**). Calculations can be found in supporting information (**Fig. S3**).

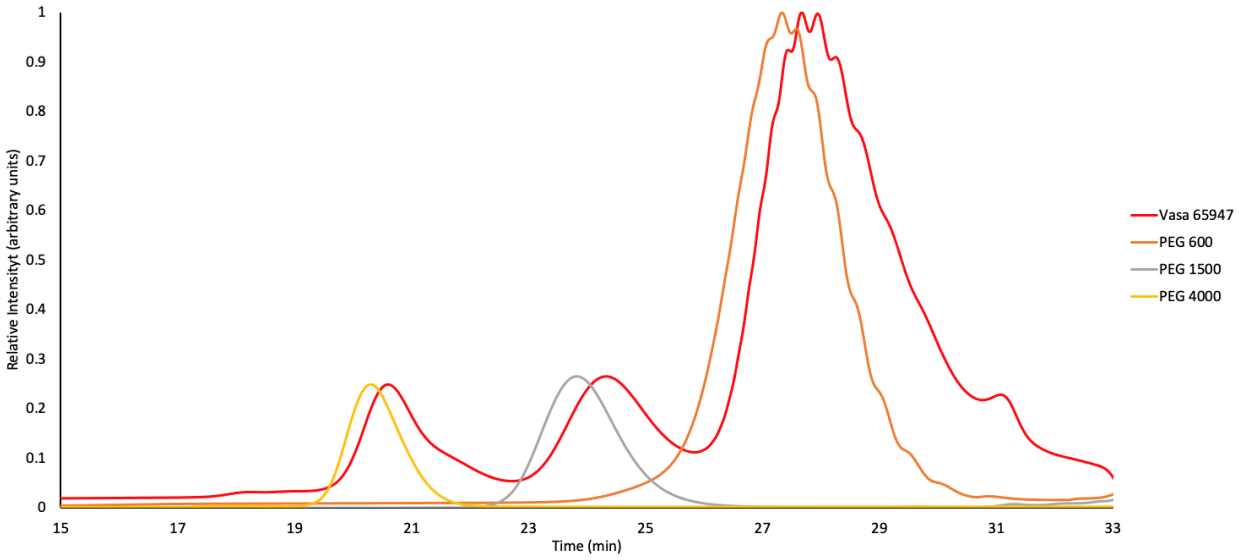

Fig. 4. GPC traces from extracted PEG sample **65947** superimposed with undegraded reference PEG 4000 Da, PEG 1500 Da, and PEG 600 Da in THF.

The 4000 Da, 1500 Da and 600 Da molecular weight ranges exhibited an average 32.6 ± 2.6, 24.8 ± 2.5, and 26.9 ± 4.6% respectively amongst the three samples. The GPC data in **Fig. 5** indicates that the PEG chains, regardless of molecular weight, are degrading at a similar rate.

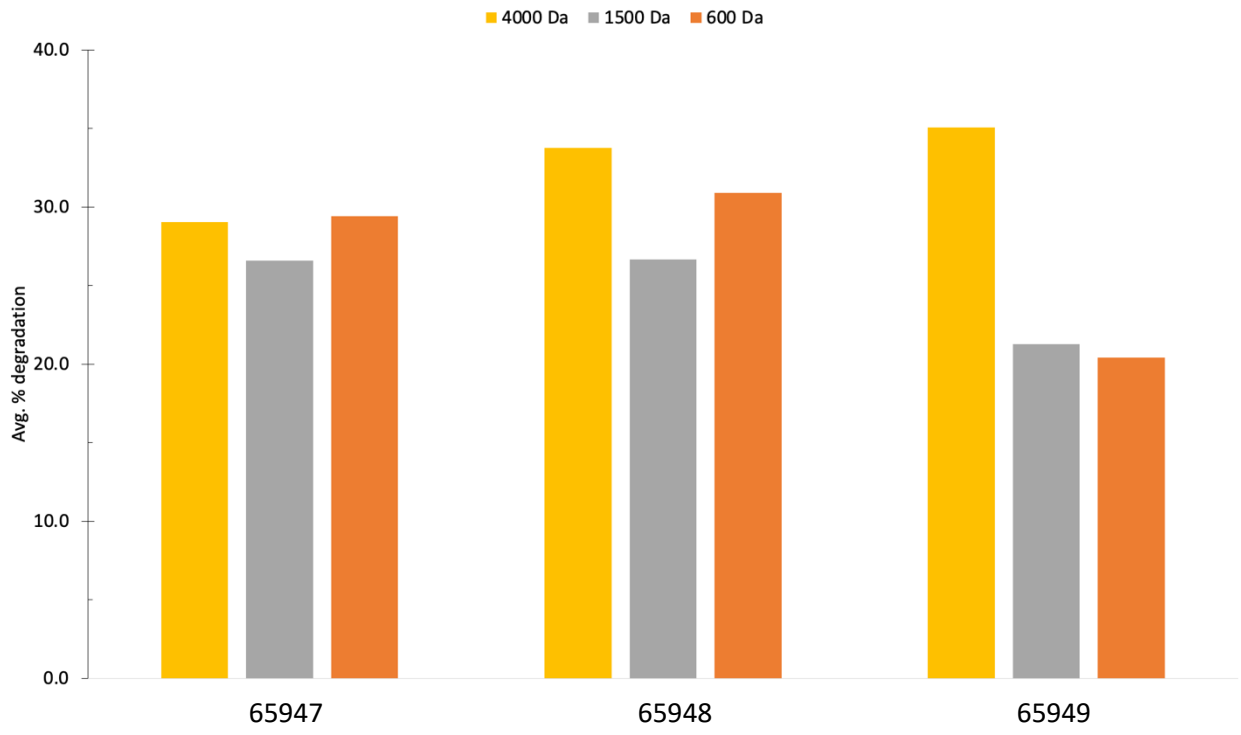

Fig. 5: Mean percent degradation of each molecular weight range (4000, 1500, and 600 Da) for each sample (**65947**- 4000 Da 29.1%, 1500 Da 26.6%, and 600 Da 29.4%; **65948**- 4000 Da 33.8%, 1500 Da 26.7%, and 600 Da 30.9%; and **65949**- 4000 Da 35.1%, 1500 Da 21.3%, and 600 Da 20.4%).

The lyophilized preservation PEG samples were qualitatively compared to both an extracted PEG, wooden sample (*Vasa* **65948**) and the reference PEG samples (**Fig. 6, S4**, and **S5**) via GPC. Each preservation PEG sample was compared to its correspondingly labeled reference PEG standard. For example, *Vasa* **65942**: labeled as "PEG 4000 M_n" was compared with the undegraded 4000 M_n reference PEG standard (M_n of 4400 via GPC and 4220 via MALDI-TOF MS.) Looking at the 4000 Da molecular weight region, the larger low molecular weight shoulder (21-22 mins) seen in *Vasa* sample **65948** suggests that there is a much larger

degree of degradation of the PEG that was extracted from the wood when compared to the lyophilized preservation PEG samples (**65942** and **65945**). This is likely due to the large amounts of degradation from the various acids such as formic, acetic, glycolic, oxalic, and sulfuric acid contained in the timbers of the ship.[5,9,29,30] Additionally, GPC eluent fractions were collected from 16 to 20 minutes and very small amounts of higher molecular weight HO-PEG-OH was observed near 10 kDa via MALDI-TOF MS. (**Fig. S6**).

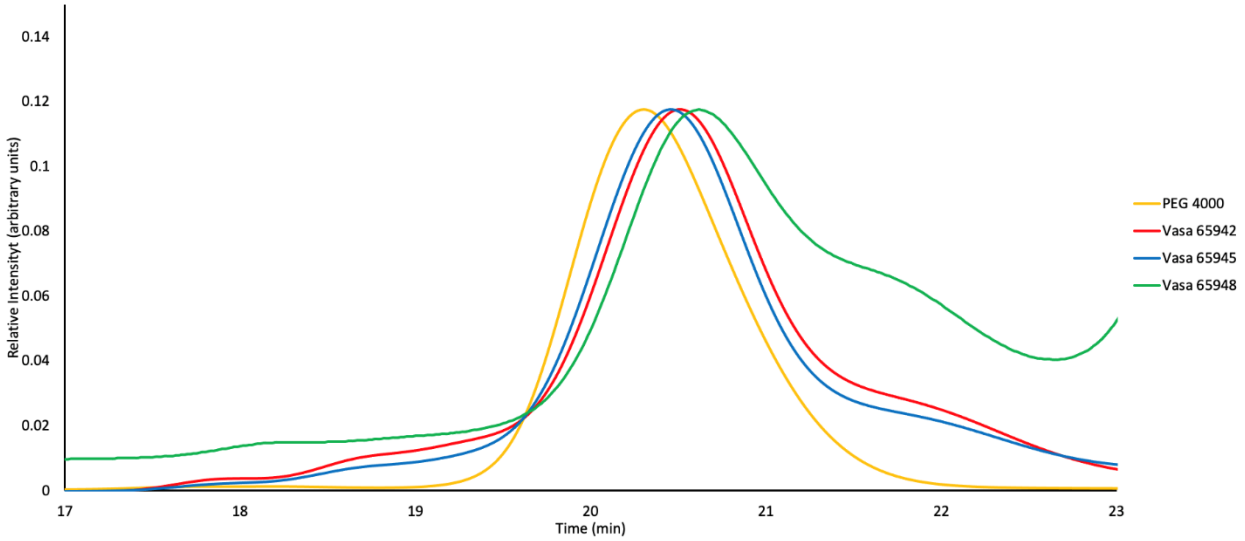

Fig. 6: GPC trace of sample **65942**: PEG 4000 ca 45%, **65945**: PEG 4000 ca 40%, **65948**, and PEG 4000 between 17 and 23 minutes of retention time in THF.

3.2 MALDI-TOF MS Data

While MALDI-TOF MS experiences low molecular weight bias in broadly dispersed samples, it is still a very powerful tool in the identification and confirmation of certain oxidative degradation products specifically at lower molecular weight. As previously mentioned, internal chain scissions are suspected to be the primary method of degradation, and a variety of PEG products with different end-groups can arise from these reactions. These species are often found in very low concentration, less than 5%, which can be an issue to interpret for analytical

techniques such as Fourier transform infrared (FTIR) spectroscopy or NMR spectroscopy, but are more easily identified via MALDI-TOF MS.

In these MALDI-TOF MS studies, the 700 to 900 Da molecular weight region was the primary focus for two reasons. First, the low molecular weight bias of MALDI-TOF MS must be considered. These extracted samples are broadly dispersed (Đ = 1.89 to 2.15), so lower molecular weight species show up more easily and exhibit significantly better isotopic resolution when compared to higher molecular weights. Second, it is suspected that the degradation products are the result of in-chain scissions; therefore, 1500 molecular weight PEG would primarily yield polymers with an average molecular weight around 750 Da. The 0 to 500 Da molecular weight range was not used due to matrix noise issues.

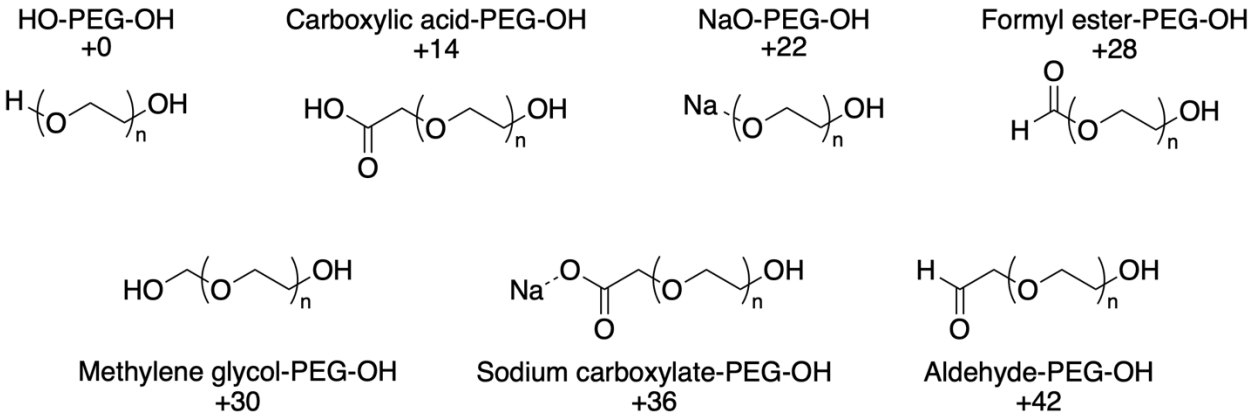

Scheme 1. Exact chemical structures and names of all the PEG species above 0.75%.

Amongst the three samples of extracted PEG, eight primary peaks were found for each repeat unit (**Fig. 7**). Their exact chemical structure is shown in **Scheme 1**. HO-PEG-OH ionizing with Na^+ (701.393 & 745.419) was the predominate species observed with 95% of the signal intensity. The remaining peaks were labeled with respect to the 701.393 (HO-PEG_{15}-OH) peak.

The +14 peak at 715.366 could correspond to an oxidation from an ether to an ester; however, selective end-group functionalizations show that it represents a carboxylic acid-PEG-OH ionizing with Na^+. The +16 peak at 717.368 could correspond to a few different things, however, K^+ counterion studies confirm that it is a HO-PEG-OH ionizing with K^+. The +22 peak at 723.378 is NaO-PEG-OH ionizing with an additional Na^+. This happens when one of the hydroxy protons of HO-PEG-OH exchanges with a Na^+ ion resulting in the +22 Da mass difference. The +28 peak at 729.386 relates to the largest initial degradation product[21] and corresponds with a formyl ester-PEG-OH ionizing with Na^+. The +30 peak at 731.395 corresponds to a methylene glycol-PEG-OH ionizing with Na^+. The +36 peak at 737.349 corresponds to sodium carboxylate-PEG-OH, a carboxylic acid-PEG-OH ionizing with Na^+ with a proton/Na^+ exchange on the carboxylic acid. This proton/Na^+ exchange shows up more intensely than the original carboxylic acid-PEG-OH in MALDI-TOF MS spectra because of the acidity of the carboxylic acid. Finally, the +42 peak at 743.402 corresponds to an aldehyde-PEG-OH.

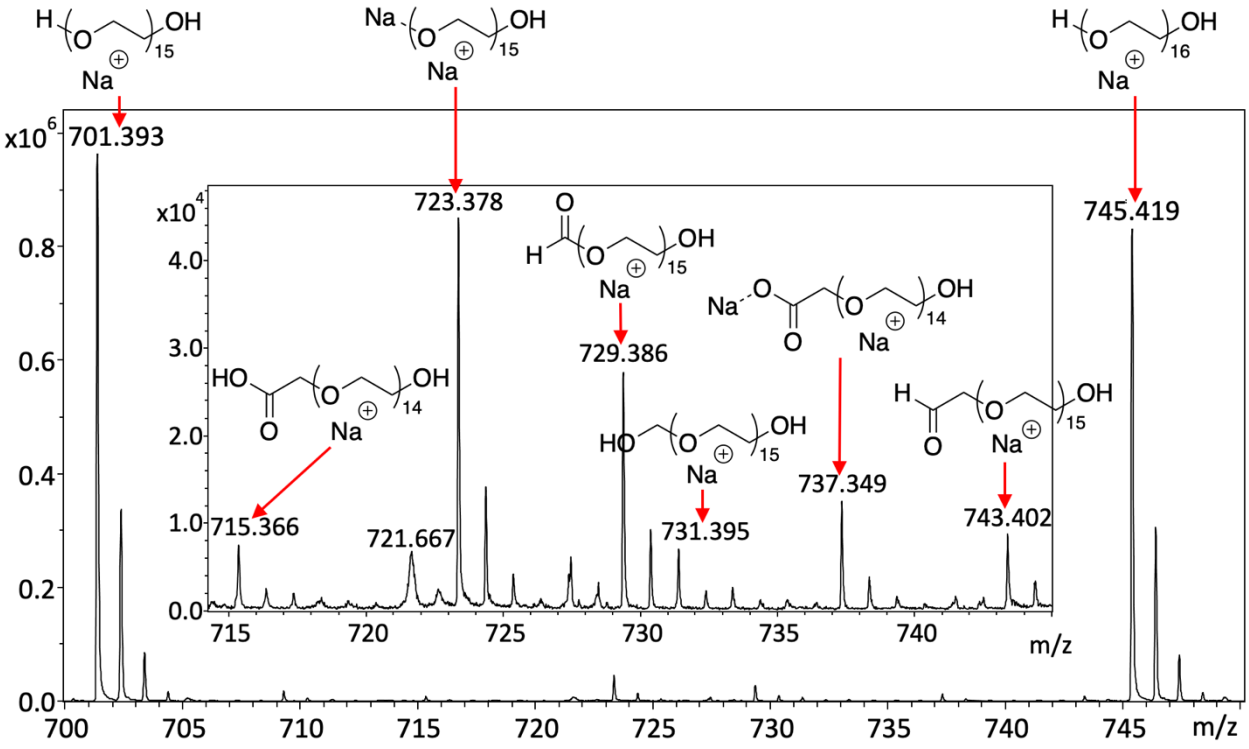

Fig. 7. MALDI-TOF MS of *Vasa* 65948 from m/z = 700 to 750 with DCTB as a matrix and Na^+ as a counter ion. The major peaks of 701.393 and 745.419 are the dihydroxy peaks (> 97%) and the minor peaks are PEG with one hydroxy group and one other end group. The peak at 721.667 is a metastable peak that is only observed in reflector mode and will be disregarded (**Fig. S19**). The inset was increased in height 20x to see the degradation peaks.

Each of the extracted samples were analyzed with the same sample preparation to ensure consistency when comparing the data. The relative intensities of the peaks were used to interpret the relative abundance of each species (**Table 3**) from 300-2200 Da to determine the overall intensities. While the species in the sample do extend above the 5000 MW range, only the dihydroxy peaks could be ascertained from above 2200 with very low amplitude and were therefore excluded.

To test the validity of the percentages in **Table 3**, analogues were made to compare the MALDI-TOF MS ionization affinities of certain PEG end-groups and how they compared to ^{1}H-NMR spectra. A modern sample of 840 M_n MeO-PEG-OH was oxidized with potassium permanganate to form MeO-PEG-carboxylic acid. The MeO-PEG-carboxylic acid was diluted incrementally from 50% down to 1% with the remaining being modern MeO-PEG-OH. These samples were analyzed via ^{1}H-NMR spectroscopy and MALDI-TOF MS. The NMR spectra integrations and MALDI-TOF MS peak integrations were compared to determine if the MALDI-TOF MS data could be used to determine concentration accurately. This procedure was also carried out for modern MeO-PEG-aldehyde (via a reaction between MeO-PEG-mesylate and monobasic sodium phosphate). At all concentrations, the MeO-PEG-carboxylic acid followed the same linear trend in both ^{1}H-NMR spectra and MALDI-TOF MS (**Fig. S7**). This, however, was not the case for the aldehyde end-group. From 2-10% the MALDI-TOF MS data of the MeO-PEG-aldehyde PEG followed an exponential trend line and produced lower than anticipated integrations when compared to the ^{1}H-NMR spectra integrations (**Fig. S8**).

According to MALDI-TOF MS data, the primary end-group species amongst the three extracted samples is HO-PEG-OH (76.85 to 93.36%). It appears that *Vasa* sample 65947 experienced the largest amount of oxidative PEG degradation. We believe this can be attributed to the location from which the samples were removed. **Fig. 1** indicates that sample 65947 had the largest exposed surface area. It seems like external sources of oxidation (light, exposure to atmosphere, and possible metal contaminants on the surface of the wood) contribute more heavily to the degradation of the PEG than internal sources (formic, acetic, glycolic, oxalic, and sulfuric acid produced in the wood of the ship) and therefore the sample with the largest external surface area would have the largest opportunity to experience degradation. In regard to possible

metal contaminants, *Vasa* samples (**65942** – **65945**) were recirculated and reused a number of times in the preservation process. Due to this recirculation, it is possible that metal ion contaminants from iron containing parts of the ship were spread amongst the surface of the rest of the ship.

Sample	Range (Da)	+14 & +36 Carboxylic acid-PEG-OH & Sodium carboxylate-PEG-OH	+28 Formyl ester-PEG-OH	+30 Methylene glycol-PEG-OH	+42 Aldehyde-PEG-OH	+0, +16, & +22 HO-PEG-OH & NaO-PEG-OH
Vasa 65947	400-2200	3.79	15.56	2.74	1.06	76.85
Vasa 65948	400-2200	3.49	2.95	1.24	1.73	90.58
Vasa 65949	400-2200	3.72	1.22	0.94	0.76	93.36

Table 3. Percent composition of each species: +14 & +36: carboxylic acid-PEG-OH & sodium carboxylate-PEG-OH, +28: formyl ester-PEG-OH, +30: methylene glycol-PEG-OH, +42: aldehyde-PEG-OH, and +0, +16, & +22: HO-PEG-OH ionizing with Na^+ or K^+ and NaO-PEG-OH in each extracted *Vasa* sample (**65947**, **65948**, and **65949**).

3.2.1 Selective End-Group Functionalizations

While each of these masses may line up with the logical, corresponding structure, how can the corresponding structures be confirmed? A combination of various selective end-group functionalizations were performed on the samples to help elucidate their functionalities.

The first selective reaction performed was the functionalization of alcohols via an esterification with acetic anhydride (**Fig. 8**). This reaction will only interact with alcohol end groups to form a methyl ester that adds 42.01 Da to compounds with only one alcohol and 84.02 Da to compounds with two alcohols. Moving from left to right amongst the peaks in the spectra (**Fig. 6**) starting with the HO-PEG-OH ionizing with sodium ($[HO\text{-}PEG_{15}\text{-}OH + Na]^+$ = 701.393 Da_{exp} and 701.393 Da_{theo}), a functionalization of both alcohols would result in the diacetate ($[CH_3COO\text{-}PEG_{15}\text{-}OCOCH_3 + Na]^+$) with a peak at 785.414 Da_{theo} (785.420 Da_{exp}). Second, the carboxylic acid-PEG-OH ($[HOCOCH_2\text{-}PEG_{14}\text{-}OH + Na]^+$ = (757.383 Da_{theo} (757.375 Da_{exp}) should gain two acetyl groups, one on the carboxylic acid side to form the anhydride and one on the alcohol side to form the ester $[CH_3COOCOCH_2\text{-}PEG_{14}\text{-}OCOCH_3 + Na]^+$ (799.393 Da_{theo} and 799.405 Da_{exp}). It should be said that after exposure to water the resulting anhydride on the carboxylic acid side can decompose leaving only one acetyl group on the alcohol, resulting in a $[HOCOCH_2\text{-}PEG_{14}\text{-}OCOCH_3 + Na]^+$ peak at 757.383 Da_{theo} (757.375 Da_{exp}) that overlaps with the $[CH_3COO\text{-}PEG_{14}\text{-}OCOCH_3 + K]^+$ peak. Third, the HO-PEG-OH ionizing with potassium ($[HO\text{-}PEG_{15}\text{-}OH + K]^+$ = 717.367 Da_{theo} (717.368 Da_{exp}) should undergo functionalizations on both alcohols, resulting in two additions of acetate groups, would result in a $[CH_3COO\text{-}PEG_{15}\text{-}OCOCH_3 + K]^+$ peak and a shift to 801.388 Da_{theo} (801.402 Da_{exp}). Fourth, the NaO-PEG-OH undergoing a proton exchange with sodium and ionizing with sodium ($[HO\text{-}PEG_{15}\text{-}O + 2Na]^+$ (723.375 Da_{theo} and 723.378 Da_{exp}) would experience two esterifications and would result in the same shift as the 701.393 ($[HO\text{-}PEG_{15}\text{-}OH + Na]^+$) peak because there is no longer a free alcohol to exchange with when collecting the MALDI-TOF MS spectra. Fifth, the formyl ester-PEG-OH ($[HCO\text{-}PEG_{15}\text{-}OH + Na]^+$ 729.388 Da_{theo} and 729.386 Da_{exp}) would undergo one functionalization (with the alcohol) resulting in a peak for acetate-PEG-formyl ester ($[CH_3COO$-

PEG_{15}-COH + $Na]^+$) at 771.398 Da_{theo} (771.402 Da_{exp}). Sixth, the methylene glycol-PEG-OH ($[HOCH_2$-PEG_{15}-OH + $Na]^+$ 731.403 Da_{theo} and 731.395 Da_{exp}) has two alcohols which can be functionalized and would result in two esterifications and a product peak for another diacetate ester ($[CH_3COO$-PEG_{15}-OCH_2OCOCH_3 + $Na]^+$) at 815.425 Da_{theo} (815.424 Da_{exp}). Seventh, the sodium carboxylate-PEG-OH undergoing a proton exchange with sodium and ionizing with sodium ($[OCOCH_2$-PEG_{14}-OH + $2Na]^+$ 737.354 Da_{theo} and 737.349 Da_{exp}), similarly to the carboxylic acid-PEG-OH, should gain two acetyl groups, one on the carboxylic acid side and one on the alcohol side, losing the ability to exchange a proton with a Na^+, resulting in the same mass species as $[CH_3COOCOCH_2$-PEG_{14}-$OCOCH_3$+ $Na]^+$ (799.393 Da_{theo} and 799.405 Da_{exp}). Last, the aldehyde-PEG-OH ($[HCOCH_2$-PEG_{15}-OH + $Na]^+$ = 743.404 Da_{theo} and 743.402 Da_{exp}) would undergo a single functionalization resulting in an ester containing peak ($[CH_3COO$-PEG_{15}-OCH_2COH $Na]^+$) at 785.414 Da_{theo} (785.420 Da_{exp}). While this functionalization does result in overlap of products in three locations, (785.414 Da (acetylation of HO-PEG_{15}-OH and aldehyde-PEG_{15}-OH), 801.402 Da (acetylation of HO-PEG_{15}-OH ionizing with K^+ and carboxylic acid-PEG_{15}-OH), and 815.424 Da (methylene glycol-PEG_{15}-OH and formyl ester-PEG_{16}-OH), all the major reactants yielded their confirmed products. Of the eight expected products from the functionalizations, all eight were confirmed.

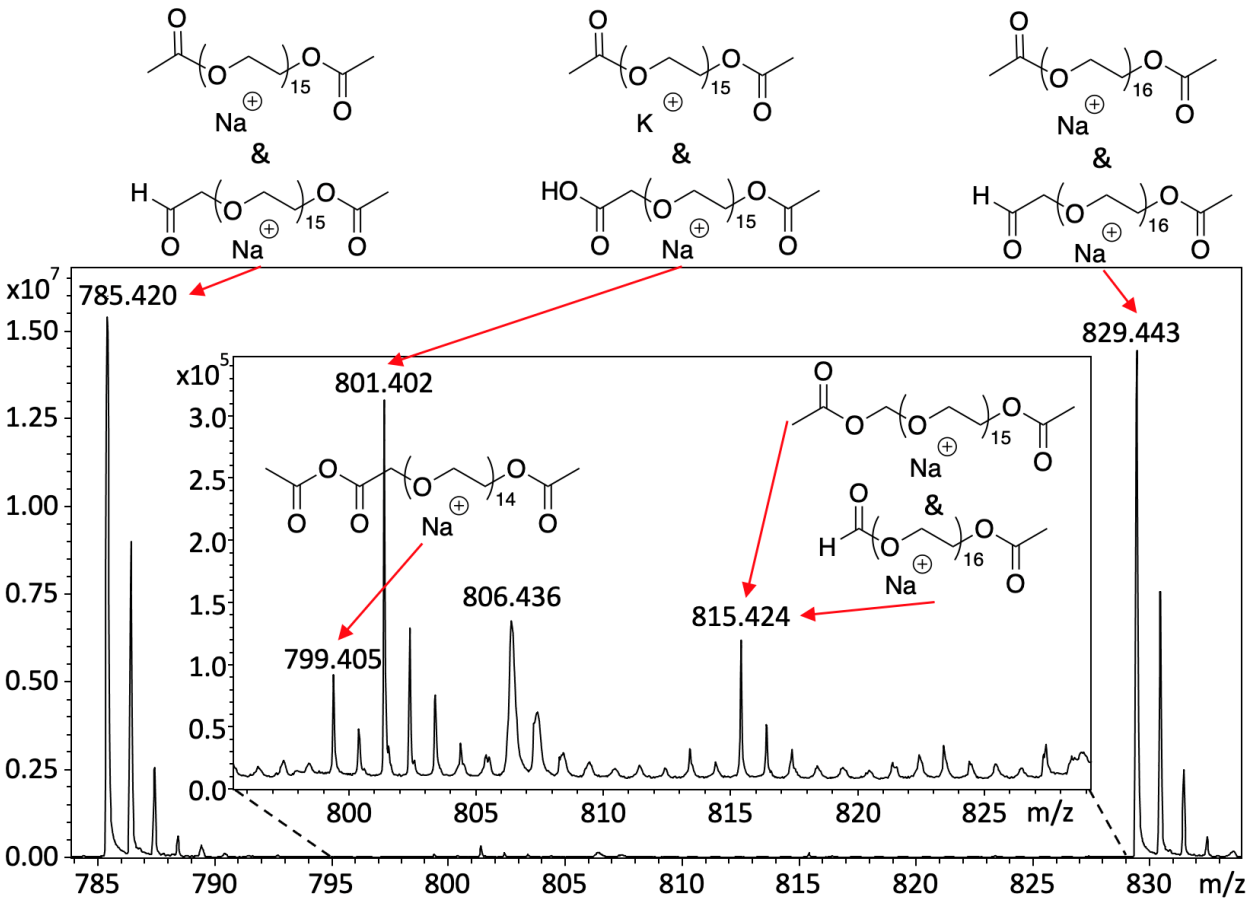

Fig. 8. MALDI-TOF MS of acetylated *Vasa* 65948 from m/z =785 to 835 with DCTB as a matrix and Na^+ as a counter ion. The major peaks are 785.420 and 829.443, the diacetyl PEGs (>99%), and the minor peaks are the functionalized PEGs with either one or two acetyl groups. The peak at 806.436 is a metastable peak that is only observed in reflector mode and will be disregarded (**Fig. S20**). The inset was increased in height 50x to see the degradation peaks.

To help confirm the mass differences seen in the esterification, a second selective functionalization was performed. Benzyl bromide was used in a Williamson ether type synthesis to functionalize both the alcohols and carboxylic acids. The addition of one benzyl group adds 90.06 Da to the total mass of the polymer while the addition of two benzyl groups will add 180.12 Da to the total mass of the polymer. It is anticipated that there will be two additions of

benzyl groups on the peaks corresponding to the HO-PEG_{15}-OH ionizing with sodium (881.487 Da_{theo}), the carboxylic acid-PEG_{14}-OH (895.466 Da_{theo}), the HO-PEG_{15}-OH ionizing with potassium (897.461 Da_{theo}), and the methylene glycol-PEG_{15}-OH (911.497 Da_{theo}) and one addition to the formyl ester-PEG_{15}-OH (819.435 Da_{theo}) and the aldehyde-PEG_{15}-OH (833.451 Da_{theo}). Furthermore, the presence of these benzyl groups eliminates any opportunity for salt/proton exchange on alcohols or carboxylic acids during the MALDI-TOF MS experiment because the most acidic protons of either the carboxylic acid or alcohol end groups are no longer present for the exchange. This means that no peaks for these proton exchange species should be present in the spectra. **Fig. 9** displays the shifted masses of the species of interest. As anticipated, the expected peaks are present in the spectra. The products that had the addition of two benzyl groups on the peaks include HO-PEG_{15}-OH ionizing with sodium (881.488 Da_{exp}), the carboxylic acid-PEG_{14}-OH (895.470 Da_{exp}) the HO-PEG_{15}-OH ionizing with potassium (897.465 Da_{exp}), and the methylene $glycol_{15}$-PEG-OH (911.491 Da_{exp}). The products with one addition of a benzyl group include the formyl ester-PEG_{15}-OH (819.440 Da_{exp}) and the aldehyde-PEG_{15}-OH (833.445 Da_{exp}). Furthermore, the peaks corresponding to the various salt/proton exchanges are not present.

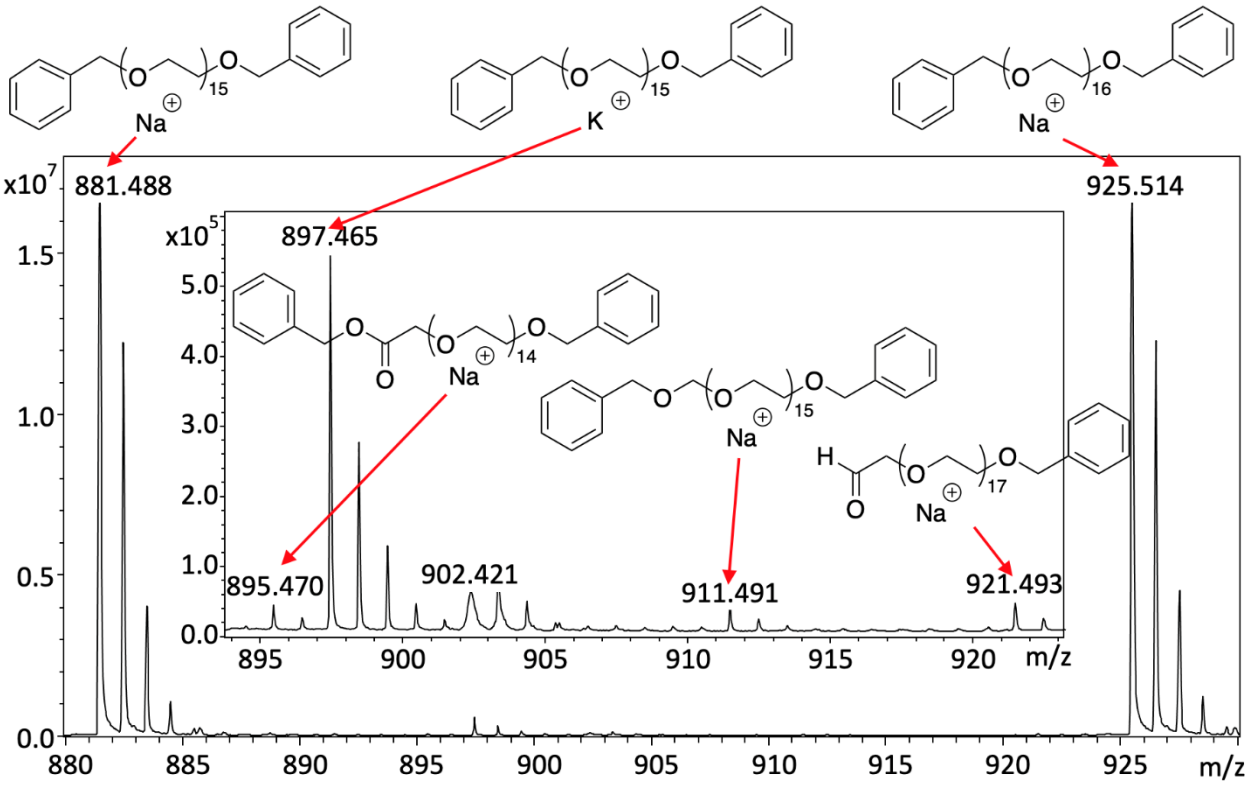

Fig. 9. MALDI-TOF MS spectra of *Vasa* **65848** from m/z = (880-935) functionalized with benzyl bromide via a Williamson ether synthesis. The major product is the debenzylated ether (>99%) from 881.488 and 925.514, with the minor peaks having one or two benzylations. The peak at 902.421 is a metastable peak that is only observed in reflector mode and will be disregarded (**Fig. S21**). The inset was increased in height 30x to see the degradation peaks.

3.3 NMR Spectroscopy Data

Proton (^{1}H) and carbon (^{13}C) NMR spectroscopy were used to analyze the three samples extracted from the wood of *Vasa* (**65947**, **65948**, and **65949**) (**Figs. 10, S9, 10, S11, S12,** and **S13**). NMR spectroscopy is a particularly useful tool due to its ability to see the entirety of the hydrogen or carbon nuclei at once. However, two issues do present themselves for looking at the chloroform extracted samples of wood. First, chloroform can extract the polyethylene glycol, but

other organic media may be included in the polyethylene glycol samples (8-12% via ^{1}H-NMR spectra integrations). Second, the end groups of polymers typically represent only a small portion of the integration of the total polymer, and when all the degradation peaks only make up 5-15% by MALDI-TOF MS (**Table 3**) of the total end groups in the sample, these peaks will be extremely small in the NMR spectra and therefore can only offer suggestions to their actual concentrations.

Proton (^{1}H) and carbon (^{13}C) NMR spectra for the extracted *Vasa* samples were run in deuterated chloroform. Peaks were characterized through ^{1}H-NMR spectroscopy; however, the primary indicator of the presence of oxidative products should be the carbonyl carbons (160 to 220 ppm) present in the end-groups. The methylenes adjacent to the ether linkages in PEG show up as a broad accumulation of peaks between 3.58 and 3.65 ppm. The terminal alcohols of dihydroxy PEG show a broad peak at 3.05 ppm and the disappearance of this peak when the ^{1}H-NMR spectra were run in D_2O or in a mixture of $CDCl_3$ and CD_3OD (**Fig. S14**) is due to proton deuterium exchange with the solvent. Of the end groups with integrable protons within their structure, the following peaks were expected: one proton from the carboxylic acid, one proton from the formyl ester, two protons from the methylene glycol, and one proton from the aldehyde. When looking at the ^{1}H-NMR spectrum of the extracted *Vasa* sample, **65947** (**Fig. 10**), the peak between 10 and 12 ppm was not present, which should be the acidic proton from the carboxylic acid; however, this is not an uncommon issue when trying to view the proton bonded to the oxygen in a carboxylic acid. This issue is also shown with the acidic proton peak for the modern carboxylic acid functionalized PEG that was functionalized for the MALDI concentration study (**Fig. S15**). It appears that the presence of water in the deuterated chloroform influences the chemical shift of the acidic carboxylic acid proton by moving it further upfield, closer to where

water typically falls (1.5 ppm) in deuterated chloroform. On the other hand, the protons of the methylene directly adjacent to the carbonyl carbon of the carboxylic is present at 4.10 ppm (∫ = 0.006), and the peak for the carbonyl carbon of the carboxylic acid end group is present at 172.9 ppm, which were confirmed by the modern carboxylic acid sample. As for the formyl ester, a peak can be seen at 8.05 ppm (∫ = 0.024) and a smaller adjacent formic acid peak at 8.08 ppm (∫ = 0.002). The carbon of the carbonyl of the formyl ester is present at 161 ppm and the carbon from the formic acid is just down field of it at 162 ppm. This formic acid peak being a byproduct of the degradation of the formyl ester group. The methylene near the formyl ester is present as a triplet at 4.28 ppm (∫ = 0.044) with an integration roughly double (as expected) as the integration of the formyl ester proton. A peak at 5.27 ppm represents the methylene that is sandwiched between the two oxygens of the methylene glycol (∫ = 0.003), and the expected methylene adjacent to this would be lost in the collection of internal PEG peaks at roughly 3.7 ppm. Lastly, the proton on the carbonyl carbon of the aldehyde produces a ^{1}H-NMR spectrum peak at 9.69 ppm (∫ = 0.001) as confirmed also by the modern aldehyde NMR spectrum, but no discernable peak in ^{13}C-NMR spectrum even when the concentration of the sample is roughly 300 mg/mL (but the ^{13}C-NMR spectrum signal only has ~1% of the ^{1}H-NMR signal). The expected methylene adjacent to this peak would be hidden under the broad OH peak near 3.05 ppm.

When these peaks are compared to the MALDI-TOF MS data, a similar trend can be seen in the concentrations of each species. For extracted *Vasa* sample **65947**, the percentages of polymers with carboxylic acids, formyl esters, methylene glycols, and aldehydes were 3.79, 15.56, 2.74, and 1.06, respectively. The ^{1}H-NMR spectra values were 0.3, 2.4, 0.15, and 0.1% respectively. The values for MALDI-TOF MS and ^{1}H-NMR spectra follow a similar

proportionality trend where the formyl esters are the most common, followed by the carboxylic acids in second, the methylene glycols in third, and the aldehydes are the least common.

Upfield from the carbonyl carbon range, there are several unassigned peaks in each of the samples from 10 to 40 ppm in the ^{13}C-NMR spectrum. According to HSQC data, (**Fig. S16)** these carbon peaks all correspond with protons in the 0.5 to 2.3 ppm region. This suggests that all these peaks can be attributed to alkanes and similar materials. It is likely that these other species were also extracted from the wooden samples during the Soxhlet extraction. *Vasa* sample **65949** was precipitated into cold diethyl ether and passed through a fritted funnel. After precipitation and filtration, the ^{1}H-NMR spectrum of the filtrate displayed significantly fewer peaks in the 0 to 2.5 ppm range of ^{1}H-NMR spectrum and the 0 to 50 ppm region for ^{13}C-NMR spectrum. This suggested that these impurities are not a part of the PEG itself but other material that were removed from the wood in the Soxhlet extraction process (**Figs. S17 and S18**).

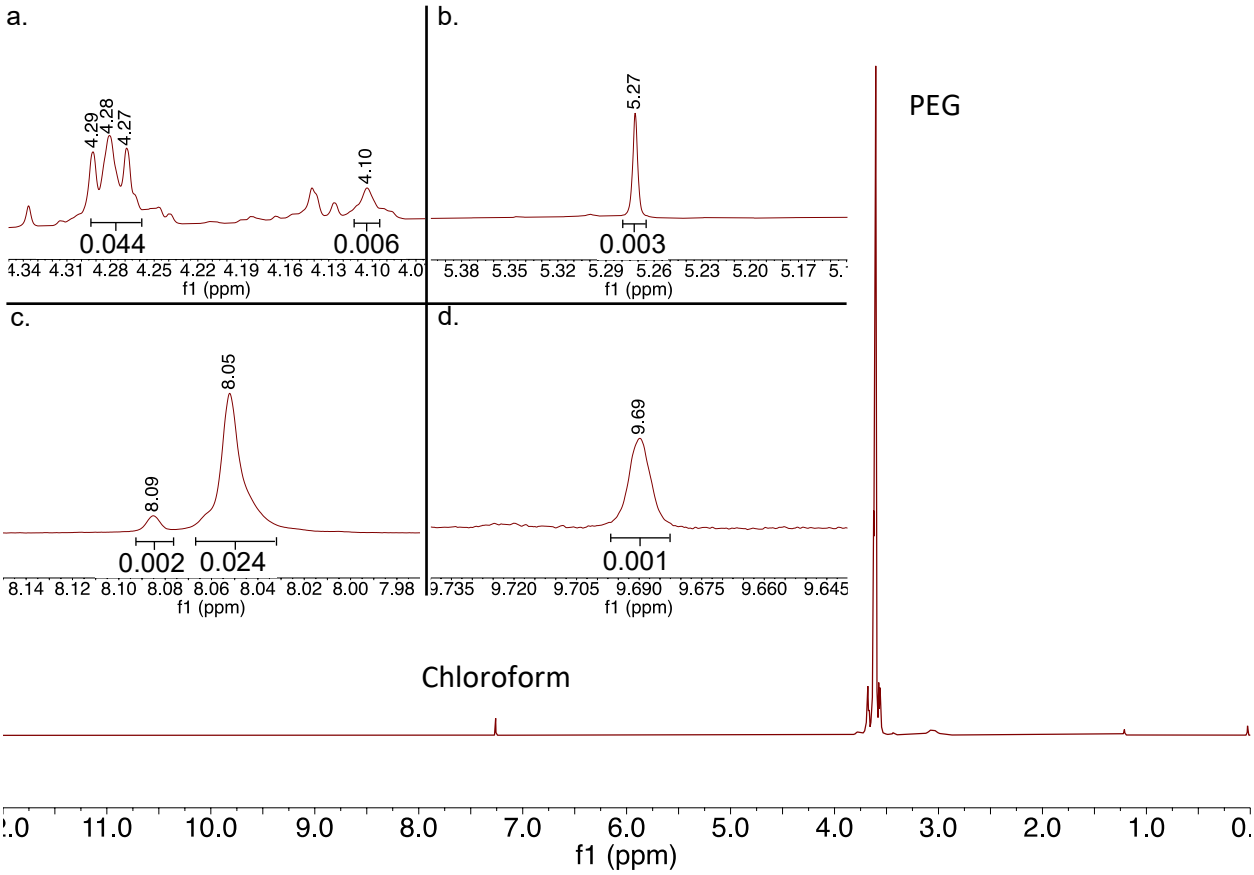

Fig. 10. ^{1}H-NMR spectrum of relevant peaks *Vasa* sample **65947** in $CDCl_3$ a. The methylene directly adjacent to the carbonyl carbon of the at 4.10 ppm ($\int$ = 0.006), and the methylene near the formyl ester is present as a triplet at 4.28 ppm ($\int$ = 0.044). b. The methylene that is sandwiched between the two oxygens of the methylene glycol at 5.27 ppm ($\int$ = 0.003). c. The proton on the carbonyl carbon of the formyl ester 8.05 ppm ($\int$ = 0.024) and the proton on the carbonyl carbon of the formic acid peak at 8.08 ppm ($\int$ = 0.002). d. The proton on the carbonyl carbon of the aldehyde at 9.69 ppm ($\int$ = 0.001).

3.4 Mechanisms of Degradation

The primary mechanism of degradation of the PEG in *Vasa* is believed to initiate with the addition of a radical followed by an oxidation. After rearrangement, and a successive oxidative

cleavage, the polymer will then have other end groups rather than the initial two OHs. These cleavages often lead to two smaller polymer chains that are roughly half the molecular weight of the parent HO-PEG-OH.[21] The major isomer and related byproducts is the formation of the formyl ester-PEG-OH and methylene glycol-PEG-OH chains. In this mechanism, a hydroperoxy group is formed which can rearrange to produce the formyl ester-PEG-OH and methylene glycol-PEG-OH.[31–33] Both end-groups can degrade further leading to a disproportionate ratio of one to another depending on their reactivities. The labile hemiacetal of the methylene glycol-PEG-OH can be further degraded into formaldehyde resulting in a lower molecular weight HO-PEG-OH, and the formyl ester-PEG-OH can further break down into a formic acid and a lower molecular weight HO-PEG-OH (**Scheme 3**). It seems that the reactivity of the hemiacetal to the HO-PEG-OH is greater than that of the formyl ester, leading to a significantly smaller amount of the methylene glycol-PEG-OH than the formyl ester-PEG-OH. This can be observed in both MALDI-TOF MS (**Table** 3) and NMR spectra.[34] Additionally, the formic acid byproduct can be seen in both ^{1}H and ^{13}C-NMR spectra, but the formaldehyde peaks are not present. This is due to their relative boiling points being 100.8 and -19˚C, respectively which assures that the formaldehyde completely evaporates while some of the formic acid remains in the sample.

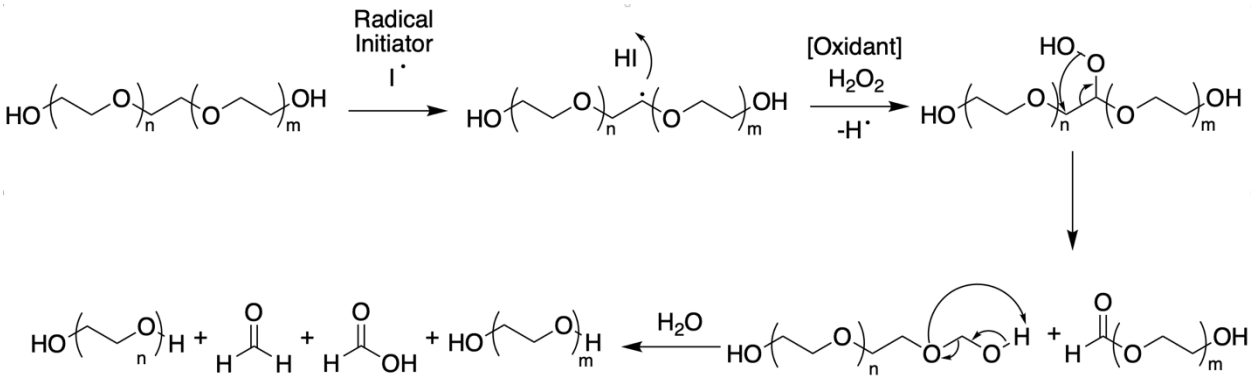

Scheme 2: Formation of formyl ester-PEG-OH and methylene glycol-PEG-OH, which then degrades to lower molecular weight HO-PEG-OH plus the formic acid and formaldehyde.

One of the minor byproducts is the carboxylic acid-PEG-OH which is formed when an in-chain ester, produced by the dehydration of the hydroperoxy group,[31,32,35–37] is hydrolyzed resulting in the formation of one carboxylic acid-PEG-OH and one HO-PEG-OH chain (**Scheme 2**). It appears that the ester hydrolysis happens very quickly after its formation resulting in only the carboxylic acid-PEG-OH and HO-PEG-OH species being present.

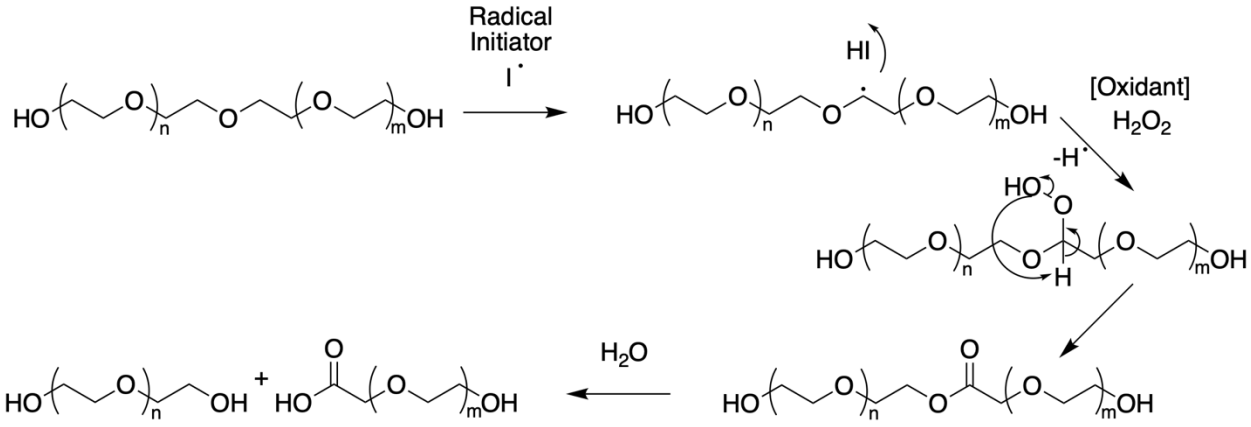

Scheme 3: Formation of ester, which then degrades to the lower molecular weight HO-PEG-OH and the carboxylic acid-PEG-OH.

The second minor byproduct is the aldehyde-PEG-OH formation, in which the polymer chain is functionalized with a hydroperoxy group, but instead of rearrangement or dehydration, it is reduced by iron species, within the ship's timbers, to a radical and recombines with a hydrogen radical to form the hemiacetal. The internal hemiacetal then undergoes a rearrangement resulting in the formation of one aldehyde-PEG-OH and one HO-PEG-OH chain (**Scheme 4**).[38,39] This reaction seems relatively unfavorable due to the lack of internal hemiacetal seen in the MALDI-TOF spectra and the proportionally small aldehyde-PEG-OH peaks observed in both the MALDI-TOF MS (**Table 3**) and NMR spectra (**Fig. 10**).

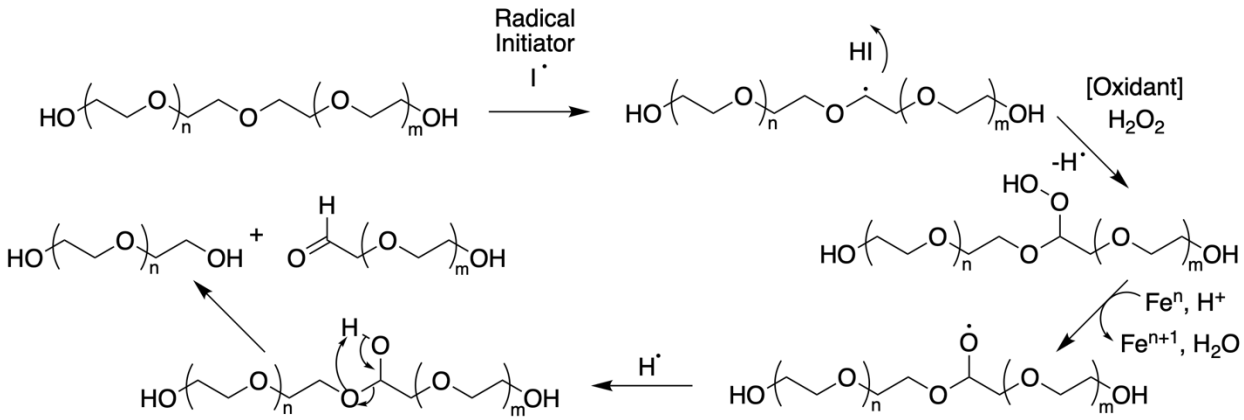

Scheme 4: Formation of hemiacetal, which then degrades to the lower molecular weight HO-PEG-OH and the aldehyde-PEG-OH.

Conclusion

In this paper, different analytical methods, GPC, NMR spectroscopy, and MALDI-TOF MS, were utilized to observe the oxidative degradation of PEG samples from the Swedish warship *Vasa.* Data has shown both the degree of degradation and the products of that degradation over the past 60 years. It was found that there has been very mild degradation of the PEG since its application as a preservation agent. By employing GPC, it was discovered that the majority of these degradative products are lower molecular weights of dihydroxy PEG that were cleaved throughout their backbones, and with the help of NMR spectroscopy and MALDI-TOF MS it was discovered that through oxidative degradation, low concentrations of PEG chains containing only a few percent of carbonyl-based end groups were formed over the last 60 years. These findings are in agreement with previous investigations on PEG from the conservation of Vasa and wooden objects.

Acknowledgements

S.M.G. acknowledges the NSF-MRI 2319960 for the MALDI-TOF MS and B.J.C. acknowledges the Louisiana Board of Regents fellowship.

References:

(1) Mahoney, M. J.; Anseth, K. S. Three-Dimensional Growth and Function of Neural Tissue in Degradable Polyethylene Glycol Hydrogels. *Biomaterials* **2006**, *27* (10), 2265–2274. https://doi.org/10.1016/j.biomaterials.2005.11.007.
(2) Fruijtier-Pölloth, C. Safety Assessment on Polyethylene Glycols (PEGs) and Their Derivatives as Used in Cosmetic Products. *Toxicology* **2005**, *214* (1), 1–38. https://doi.org/10.1016/j.tox.2005.06.001.
(3) Phan, T. N.; Issa, S.; Gigmes, D. Poly(Ethylene Oxide)-Based Block Copolymer Electrolytes for Lithium Metal Batteries. *Polym. Int.* **2019**, *68* (1), 7–13. https://doi.org/10.1002/pi.5677.
(4) Hocker, E.; Almkvist, G.; Sahlstedt, M. The Vasa Experience with Polyethylene Glycol: A Conservator's Perspective. *J. Cult. Herit.* **2012**, *13* (3, Supplement), S175–S182. https://doi.org/10.1016/j.culher.2012.01.017.
(5) Almkvist, G.; Persson, I. Analysis of Acids and Degradation Products Related to Iron and Sulfur in the Swedish Warship Vasa. **2008**, *62* (6), 694–703. https://doi.org/10.1515/HF.2008.130.
(6) Almkvist, G.; Persson, I. Degradation of Polyethylene Glycol and Hemicellulose in the Vasa. **2008**, *62* (1), 64–70. https://doi.org/10.1515/HF.2008.009.
(7) Mortensen, M. N.; Egsgaard, H.; Hvilsted, S.; Shashoua, Y.; Glastrup, J. Characterisation of the Polyethylene Glycol Impregnation of the Swedish Warship Vasa and One of the Danish Skuldelev Viking Ships. *J. Archaeol. Sci.* **2007**, *34* (8), 1211–1218. https://doi.org/10.1016/j.jas.2006.10.012.
(8) Glastrup, J.; Shashoua, Y.; Egsgaard, H.; Mortensen, M. N. Degradation of PEG in the Warship Vasa. *Macromol. Symp.* **2006**, *238* (1), 22–29. https://doi.org/10.1002/masy.200650604.
(9) Glastrup, J.; Shashoua, Y.; Egsgaard, H.; Mortensen, M. N. Formic and Acetic Acids in Archaeological Wood. A Comparison between the Vasa Warship, the Bremen Cog, the Oberländer Boat and the Danish Viking Ships. **2006**, *60* (3), 259–264. https://doi.org/10.1515/HF.2006.042.
(10) Hoffmann, P. To Be and to Continue Being a Cog: The Conservation of the Bremen Cog of 1380. *Int. J. Naut. Archaeol.* **2001**, *30* (1), 129–140. https://doi.org/10.1016/S1057-2414(01)80015-7.

(11) Hoffmann, P.; Singh, A.; Kim, Y. S.; Wi, S. G.; Kim, I.-J.; Schmitt, U. The Bremen Cog of 1380 – An Electron Microscopic Study of Its Degraded Wood before and after Stabilization with PEG. **2004**, *58* (3), 211–218. https://doi.org/10.1515/HF.2004.033.
(12) Hoffmann, P. On the Long-Term Visco-Elastic Behaviour of Polyethylene Glycol (PEG) Impregnated Archaeological Oak Wood. **2010**, *64* (6), 725–728. https://doi.org/10.1515/hf.2010.082.
(13) Preston, J.; Smith, A. D.; Schofield, E. J.; Chadwick, A. V.; Jones, M. A.; Watts, J. E. M. The Effects of Mary Rose Conservation Treatment on Iron Oxidation Processes and Microbial Communities Contributing to Acid Production in Marine Archaeological Timbers. *PLOS ONE* **2014**, *9* (2), e84169. https://doi.org/10.1371/journal.pone.0084169.
(14) Chadwick, A. V.; Berko, A.; Schofield, E. J.; Smith, A. D.; Mosselmans, J. F. W.; Jones, A. M.; Cibin, G. The Application of X-Ray Absorption Spectroscopy in Archaeological Conservation: Example of an Artefact from Henry VIII Warship, the *Mary Rose*. *J. Non-Cryst. Solids* **2016**, *451*, 49–55. https://doi.org/10.1016/j.jnoncrysol.2016.05.020.
(15) Finney, R. W.; Jones, A. M. Direct Analysis of Wood Preservatives in Ancient Oak from the Mary Rose by Laser Microprobe Mass Spectrometry. *Stud. Conserv.* **1993**, *38* (1), 36–44. https://doi.org/10.1179/sic.1993.38.1.36.
(16) Parray, Z. A.; Hassan, M. I.; Ahmad, F.; Islam, A. Amphiphilic Nature of Polyethylene Glycols and Their Role in Medical Research. *Polym. Test.* **2020**, *82*, 106316. https://doi.org/10.1016/j.polymertesting.2019.106316.
(17) Andishmand, H.; Tabibiazar, M.; Mohammadifar, M. A.; Hamishehkar, H. Pectin-Zinc-Chitosan-Polyethylene Glycol Colloidal Nano-Suspension as a Food Grade Carrier for Colon Targeted Delivery of Resveratrol. *Int. J. Biol. Macromol.* **2017**, *97*, 16–22. https://doi.org/10.1016/j.ijbiomac.2016.12.087.
(18) Jang, H.-J.; Shin, C. Y.; Kim, K.-B. Safety Evaluation of Polyethylene Glycol (PEG) Compounds for Cosmetic Use. *Toxicol. Res.* **2015**, *31* (2), 105–136. https://doi.org/10.5487/TR.2015.31.2.105.
(19) Naskar, A.; Khan, H.; Sarkar, R.; Kumar, S.; Halder, D.; Jana, S. Anti-Biofilm Activity and Food Packaging Application of Room Temperature Solution Process Based Polyethylene Glycol Capped Ag-ZnO-Graphene Nanocomposite. *Mater. Sci. Eng. C* **2018**, *91*, 743–753. https://doi.org/10.1016/j.msec.2018.06.009.
(20) Zidan, N. S.; Aziz albalawi, M.; Alalawy, A. I.; Al-Duais, M. A.; Alzahrani, S.; Kasem, M. Modification of Edible Chitosan/Polyethylene Glycol Films Fortified with Date Palm Fruit Waste Extract as Promising Antimicrobial Food Packaging Materials for Fresh Strawberry Conservation. *Eur. Polym. J.* **2023**, *194*, 112171. https://doi.org/10.1016/j.eurpolymj.2023.112171.
(21) Payne, M. E.; Kareem, O. O.; Williams-Pavlantos, K.; Wesdemiotis, C.; Grayson, S. M. Mass Spectrometry Investigation into the Oxidative Degradation of Poly(Ethylene Glycol). *Polym. Degrad. Stab.* **2021**, *183*, 109388. https://doi.org/10.1016/j.polymdegradstab.2020.109388.
(22) Voorhees, K. J.; Baugh, S. F.; Stevenson, D. N. An Investigation of the Thermal Degradation of Poly(Ethylene Glycol). *J. Anal. Appl. Pyrolysis* **1994**, *30* (1), 47–57. https://doi.org/10.1016/0165-2370(94)00803-5.

(23) Glastrup, J. Degradation of Polyethylene Glycol. A Study of the Reaction Mechanism in a Model Molecule: Tetraethylene Glycol. *Polym. Degrad. Stab.* **1996**, *52* (3), 217–222. https://doi.org/10.1016/0141-3910(95)00225-1.
(24) *Microbial Degradation of Polyethylene Glycols*. https://doi.org/10.1128/am.29.5.621-625.1975.
(25) Bergh, M.; Magnusson, K.; Nilsson, J. L. G.; Karlberg, A.-T. Formation of Formaldehyde and Peroxides by Air Oxidation of High Purity Polyoxyethylene Surfactants. *Contact Dermatitis* **1998**, *39* (1), 14–20. https://doi.org/10.1111/j.1600-0536.1998.tb05805.x.
(26) Hamburger, R.; Azaz, E.; Donbrow, M. Autoxidation of Polyoxyethylenic Non-Ionic Surfactants and of Polyethylene Glycols. *Pharm. Acta Helv.* **1975**, *50* (1–2), 10–17.
(27) Knop, K.; Hoogenboom, R.; Fischer, D.; Schubert, U. S. Poly(Ethylene Glycol) in Drug Delivery: Pros and Cons as Well as Potential Alternatives. *Angew. Chem. Int. Ed.* **2010**, *49* (36), 6288–6308. https://doi.org/10.1002/anie.200902672.
(28) Hemenway, J. N.; Carvalho, T. C.; Rao, V. M.; Wu, Y.; Levons, J. K.; Narang, A. S.; Paruchuri, S. R.; Stamato, H. J.; Varia, S. A. Formation of Reactive Impurities in Aqueous and Neat Polyethylene Glycol 400 and Effects of Antioxidants and Oxidation Inducers. *J. Pharm. Sci.* **2012**, *101* (9), 3305–3318. https://doi.org/10.1002/jps.23198.
(29) Sandström, M.; Jalilehvand, F.; Persson, I.; Gelius, U.; Frank, P.; Hall-Roth, I. Deterioration of the Seventeenth-Century Warship Vasa by Internal Formation of Sulphuric Acid. *Nature* **2002**, *415* (6874), 893–897. https://doi.org/10.1038/415893a.
(30) Dedic, D.; Iversen, T.; Ek, M. Cellulose Degradation in the Vasa: The Role of Acids and Rust. *Stud. Conserv.* **2013**, *58* (4), 308–313. https://doi.org/10.1179/2047058412Y.0000000069.
(31) Mkhatresh, O. A.; Heatley, F. A Study of the Products and Mechanism of the Thermal Oxidative Degradation of Poly(Ethylene Oxide) Using 1H and 13C 1-D and 2-D NMR. *Polym. Int.* **2004**, *53* (9), 1336–1342. https://doi.org/10.1002/pi.1531.
(32) Mkhatresh, O. A.; Heatley, F. A 13C NMR Study of the Products and Mechanism of the Thermal Oxidative Degradation of Poly(Ethylene Oxide). *Macromol. Chem. Phys.* **2002**, *203* (16), 2273–2280. https://doi.org/10.1002/macp.200290001.
(33) Mortensen, M. N.; Egsgaard, H.; Hvilsted, S.; Shashoua, Y.; Glastrup, J. Tetraethylene Glycol Thermooxidation and the Influence of Certain Compounds Relevant to Conserved Archaeological Wood. *J. Archaeol. Sci.* **2012**, *39* (11), 3341–3348. https://doi.org/10.1016/j.jas.2012.05.032.
(34) Reid, B.; Tzeng, S.; Warren, A.; Kozielski, K.; Elisseeff, J. Development of a PEG Derivative Containing Hydrolytically Degradable Hemiacetals. *Macromolecules* **2010**, *43* (23), 9588–9590. https://doi.org/10.1021/ma1020648.
(35) Costa, L.; Gad, A. M.; Camino, G.; Cameron, G. G.; Qureshi, M. Y. Thermal and Thermooxidative Degradation of Poly(Ethylene Oxide)-Metal Salt Complexes. *Macromolecules* **1992**, *25* (20), 5512–5518. https://doi.org/10.1021/ma00046a059.
(36) Chang, T. C.; Wu, K. H.; Chen, H. B.; Ho, S. Y.; Chiu, Y. S. Thermal Degradation of Aged Polytetrahydrofuran and Its Copolymers with 3-Azidomethyl-3'-Methyloxetane and 3-Nitratomethyl-3'-Methyloxetane by Thermogravimetry. *J. Polym. Sci. Part Polym. Chem.* **1996**, *34* (16), 3337–3343. https://doi.org/10.1002/(SICI)1099-0518(19961130)34:16<3337::AID-POLA10>3.0.CO;2-H.

(37) Soto-Oviedo, M. A.; De Paoli, M.-A. Photo-Oxidative Degradation of Poly(Epichlorohydrin-Co-Ethylene Oxide) Elastomer at 254 Nm. *Polym. Degrad. Stab.* **2002**, *76* (2), 219–225. https://doi.org/10.1016/S0141-3910(02)00017-4.
(38) Almkvist, G.; Persson, I. Fenton-Induced Degradation of Polyethylene Glycol and Oak Holocellulose. A Model Experiment in Comparison to Changes Observed in Conserved Waterlogged Wood. **2008**, *62* (6), 704–708. https://doi.org/10.1515/HF.2008.129.
(39) Kerem, Z.; Bao, W.; Hammel, K. E. Rapid Polyether Cleavage via Extracellular One-Electron Oxidation by a Brown-Rot Basidiomycete. *Proc. Natl. Acad. Sci. U. S. A.* **1998**, *95* (18), 10373–10377. https://doi.org/10.1073/pnas.95.18.10373